



HAL
open science

Identification of the fatty acid coenzyme-A ligase FadD1 as an interacting partner of FptX in the *Pseudomonas aeruginosa* pyochelin pathway

Béatrice Roche, Gaëtan L.A. Mislin, Isabelle J Schalk

► To cite this version:

Béatrice Roche, Gaëtan L.A. Mislin, Isabelle J Schalk. Identification of the fatty acid coenzyme-A ligase FadD1 as an interacting partner of FptX in the *Pseudomonas aeruginosa* pyochelin pathway. FEBS Letters, inPress, 10.1002/1873-3468.14012 . hal-03039826

HAL Id: hal-03039826

<https://hal.science/hal-03039826>

Submitted on 4 Dec 2020

HAL is a multi-disciplinary open access archive for the deposit and dissemination of scientific research documents, whether they are published or not. The documents may come from teaching and research institutions in France or abroad, or from public or private research centers.

L'archive ouverte pluridisciplinaire **HAL**, est destinée au dépôt et à la diffusion de documents scientifiques de niveau recherche, publiés ou non, émanant des établissements d'enseignement et de recherche français ou étrangers, des laboratoires publics ou privés.



Identification of the fatty acid coenzyme-A ligase FadD1 as an interacting partner of FptX in the *Pseudomonas aeruginosa* pyochelin pathway

Journal:	<i>FEBS Letters</i>
Manuscript ID	FEBSL-20-1255.R1
Wiley - Manuscript type:	Research Letter
Date Submitted by the Author:	n/a
Complete List of Authors:	ROCHE, Béatrice; Universität Basel Department Biozentrum, Infection Biology Focal Area Mislin, Gaëtan; CNRS-Universite de Strasbourg, UMR7242 schalk, isabelle; CNRS-Universite de Strasbourg, UMR7242
Keywords:	<i>Pseudomonas aeruginosa</i> , pyochelin siderophore, iron uptake, coenzyme-A ligase, membrane complex
Abstract:	<p><i>Pseudomonas aeruginosa</i> is one of the most important nosocomial bacteria emerging as a highly multidrug-resistant pathogen. <i>P. aeruginosa</i> produces two siderophores including pyochelin to fulfill its need for iron during infections. We know that both outer and inner membrane proteins FptA and FptX are involved in the ferri-pyochelin uptake, but this process requires increasing molecular and biochemical knowledge. Here, using bacterial two-hybrid and copurification assays we identified the fatty acid coenzyme-A ligase FadD1 as a novel interacting partner of the inner membrane transporter FptX, and found that FadD1 may play a role in pyochelin production. We managed to purify the FadD1-FptX inner membrane complex and obtained low-resolution 3D models, opening the way for future high-resolution structures.</p>

1 **Identification of the fatty acid coenzyme-A ligase FadD1 as an interacting partner of FptX in the**
2 ***Pseudomonas aeruginosa* pyochelin pathway**

3

4 Béatrice Roche^{1,2,3*}, Gaëtan L.A. Mislin^{1,2} and Isabelle J. Schalk^{1,2}

5 ¹. CNRS, UMR7242, ESBS, Bld Sébastien Brant, F-67412 Illkirch, France.

6 ². Université de Strasbourg, UMR7242, ESBS, Bld Sébastien Brant, F-67412 Illkirch, France.

7 ³. Present address: Biozentrum, University of Basel, CH-4056 Basel, Switzerland

8 * = correspondence should be addressed to Béatrice Roche (beatrice.roche@unibas.ch)

9

10 **Abstract**

11 *Pseudomonas aeruginosa* is one of the most important nosocomial bacteria emerging as a highly
12 multidrug-resistant pathogen. *P. aeruginosa* produces two siderophores including pyochelin to fulfill its
13 need for iron during infections. We know that both outer and inner membrane proteins FptA and FptX are
14 involved in the ferri-pyochelin uptake, but this process requires increasing molecular and biochemical
15 knowledge. Here, using bacterial two-hybrid and copurification assays we identified the fatty acid
16 coenzyme-A ligase FadD1 as a novel interacting partner of the inner membrane transporter FptX, and found
17 that FadD1 may play a role in pyochelin production. We managed to purify the FadD1-FptX inner
18 membrane complex and obtained low-resolution 3D models, opening the way for future high-resolution
19 structures.

20

21

22 **Keywords:** *Pseudomonas aeruginosa*; pyochelin siderophore; iron uptake; coenzyme-A ligase; membrane
23 complex.

24

25

26

27 **Introduction**

28 *Pseudomonas aeruginosa* is a major human pathogen naturally resistant to many antibiotics due to the low
29 permeability of its envelope. The situation is particularly critical as *P. aeruginosa* belongs to the World
30 Health Organization list of antibiotic-resistant priority pathogen [1]. The success of bacteria to colonize the
31 host relies mostly on their ability to obtain adequate supplies of the nutrients that are essential for growth
32 and virulence. To circumvent the low bioavailability of iron in the host during infections, *P. aeruginosa*
33 produces the two siderophores pyoverdine (PVD) and pyochelin (PCH) [2-4]. Siderophores are small iron
34 chelating compounds produced by bacteria under iron limitation conditions [5]. Previous studies have shown
35 an upregulation of the PCH pathway in clinical isolates from cystic fibrosis patients [6-7] and reported a
36 potential role of PCH in the inflammatory response [8].

37 PCH is synthesized by non-ribosomal peptide synthetases in the bacterial cytoplasm and then secreted into
38 the extracellular medium by an unknown mechanism [9]. Once in the bacterial environment, PCH chelates
39 ferric iron leading to the formation of ferri-PCH complexes. Only two proteins involved in the ferri-PCH
40 uptake have been described so far: the specific TonB-dependent outer membrane transporter FptA [10-12],
41 and the inner membrane protein FptX [13-15]. Much attention has been paid to structural studies of FptA,
42 and X-ray structure of FptA bound to ferri-PCH provided valuable information for the design of PCH-
43 antibiotic conjugates [16-17]. In the context of antibiotic resistance, conjugation of antibiotics with
44 siderophore is a promising drug delivery strategy exploiting iron uptake systems as gates to carry out
45 antibiotics into the bacteria [18-19]. Such Trojan horse strategy can provide increased penetration of drugs
46 previously unable to cross the cell wall of bacteria [4]. But we currently lack biochemical/structural data on
47 the inner membrane transporter FptX predicted to have 12 transmembrane segments.

48 Here, we explored potential new actors involved in the ferri-PCH uptake pathway by using a genome-wide
49 screening approach. We identified the fatty acid coenzyme-A ligase FadD1 as a new and previously
50 undescribed interacting partner of FptX, forming an inner membrane complex. Deletion of *fadD1* led to a
51 decrease in PCH production, suggesting a role of FadD1 in biosynthesis and/or secretion of this siderophore.

52 We also managed to express and purify FptX and could establish low-resolution 3D models of FptX, FadD1
53 and of the FadD1-FptX complex by negative-stain electron microscopy (EM).

54

55 **Materials and methods**

56 **Chemicals and growth media.**

57 X-Gal (5-bromo-4-chloro-3-indoyl- β -D-galactopyranoside) and IPTG (Isopropyl- β -D thiogalactoside) were
58 purchased from Euromedex. ONPG (2-Nitrophenyl- β -D galactopyranoside) and sodium oleate were
59 obtained from Sigma-Aldrich. Detergent n-Dodecyl- β -D-maltopyranoside (DDM) was purchased from
60 Anatrace. LB (Lennox) and LB agar medium were both purchased from Difco and were used as nutriment-
61 rich medium in all experiments. Bacteria were routinely grown at 30°C in LB broth (Difco) or in iron-
62 restricted medium (CAA) as previously described [15]. Media were supplemented as necessary with
63 ampicillin (Ap; 100 $\mu\text{g.mL}^{-1}$), kanamycin (Kan; 50 $\mu\text{g.mL}^{-1}$), gentamicin (Gm; 30 $\mu\text{g.mL}^{-1}$),
64 chloramphenicol (Cm; 50 $\mu\text{g.mL}^{-1}$), IPTG (0.5 mM). The strains used in this study are listed in Table S1.

65

66 **Plasmids construction.**

67 All DNA amplifications for cloning were performed with Phusion High-Fidelity DNA polymerase
68 (ThermoFisher Scientific) using genomic DNA of PAO1 strain as template. Restriction enzymes and T4
69 DNA ligase were purchased from ThermoFisher Scientific. All enzymes were used in accordance with the
70 manufacturer's instructions. Oligonucleotides are listed in Table S2. *Escherichia coli* strain Top10 was used
71 as the host strain for all plasmids. Absence of mutations was checked by DNA sequencing (GATC).

72 *Expression plasmids.* Plasmid p33-fptX(His₆) was constructed by PCR amplification of the coding region
73 of *fptX* by using the primer pairs 970/969. The PCR product was then digested with EcoRI and HindIII
74 enzymes and ligated into the EcoRI/HindIII linearized pBAD33 vector. Plasmid p24-fadD1(StrepII) was
75 constructed by PCR amplification of the coding region of *fadD1* by using the primer pairs 1157/1158. The
76 PCR product was then digested with NcoI and HindIII enzymes and ligated into the NcoI/HindIII linearized
77 pBAD24 vector.

78 *Two-hybrid plasmids.* DNA fragments encoding proteins of interest were fused to the two fragments T25
79 and T18 of *Bordetella pertussis* adenylate cyclase carried on the pKT25, pKNT25, pUT18C and pUT18
80 vectors. The DNA regions encoding *fptX* and *fadD1* were amplified by PCR by using primer pairs 951/952
81 and 1037/1038, respectively. PCR products were then digested with XbaI and KpnI enzymes and ligated
82 into the XbaI/KpnI linearized pKT25, pKNT25, pUT18C and pUT18 vectors.

83

84 **Bacterial two-hybrid screen.**

85 Four independent two-hybrid libraries (pUT18CPAO1Lib, pUT18PAO1Lib, pUT18+1PAO1Lib and
86 pUT18+2PAO1Lib) of PAO1 genome were tested independently. The pKNT25-fptX vector was used as
87 the bait and the two-hybrid screen was performed as described in Houot *et al.*, 2012 [20].

88

89 **Bacterial two-hybrid assay.**

90 The adenylate cyclase-based bacterial two-hybrid technique was used as previously published [21].

91

92 **Western blot analysis.**

93 Proteins were applied to SDS-PAGE acrylamide gels and transferred onto nitrocellulose membranes.
94 FptX(His₆) and FadD1(StrepII) proteins were immunodetected with the anti-His (1:3,000 ; GeneTex) and
95 the StrepMAB (1:1,000 ; IBA) antibodies, respectively. Immunoblots were developed by using horseradish
96 peroxidase-conjugated goat anti-rabbit and anti-mouse antibodies (1:10,000 ; GE Healthcare), followed by
97 chemiluminescence detection.

98

99 **Expression and purification of FptX.**

100 Top10 *E. coli* cells were transformed with the p33-fptX(His₆) vector. Cells were grown at 37°C with shaking
101 until they reached an OD₆₀₀ ≈ 0.5, and the expression of *fptX* gene was induced with 0.01 % arabinose for
102 4 h at 37°C. Cell pellets were resuspended in 50 mM Tris-HCl pH 8, 100 mM NaCl, supplemented with
103 EDTA-free protease inhibitor (Roche). After sonication, the cell suspension was clarified by centrifugation

104 at 7,700 g for 15 min at 4°C. Membrane fraction was then collected by ultracentrifugation at 118,000 g for
105 40 min at 4°C. After mechanically homogenized, membranes were solubilized in 50 mM Tris-HCl pH 8,
106 200 mM NaCl, 1 % DDM at 4°C overnight. The suspension was clarified by ultracentrifugation at
107 118,000 g for 40 min at 4°C. The supernatant was loaded onto a 1-mL HisTrap HP column (GE Healthcare)
108 equilibrated with buffer A (50 mM Tris-HCl pH 8, 500 mM NaCl, 0.1 % n-Dodecyl- β -D-maltopyranoside
109 (DDM), 20 mM imidazole). FptX was eluted in buffer A containing 500 mM imidazole. Central fraction of
110 the peak was loaded onto a Superdex 200 10/300 GL column (GE Healthcare) equilibrated with 50 mM
111 Hepes pH 7.5, 50 mM NaCl, 0.025 % DDM. FptX was eluted as a single peak and the central fraction was
112 immediately used for EM sample preparation.

113

114 **Expression and purification of FadD1.**

115 Top10 *E. coli* cells were transformed with the p24-fadD1(StrepII) vector. Cell growth, gene induction and
116 membrane preparation were done as described for FptX. The supernatant was loaded onto a 5-mL StrepTrap
117 HP column (GE Healthcare) equilibrated with buffer A (50 mM Tris-HCl pH 8, 200 mM NaCl, 0.1 %
118 DDM). FadD1 was eluted in buffer A containing 2.5 mM D-Desthiobiotin. Peak fractions were pooled and
119 loaded onto a Superdex 200 10/300 GL (GE Healthcare) column equilibrated with 50 mM Hepes pH 7.5,
120 50 mM NaCl, 0.025 % DDM. FadD1 was eluted as a single peak and the central fraction was immediately
121 used for EM sample preparation.

122

123 **Expression and purification of the FadD1-FptX complex by two-step affinity chromatography.**

124 Top10 *E. coli* cells were transformed with the p33-fptX(His₆) and p24-fadD1(StrepII) vectors. Cell growth,
125 gene induction and membrane preparation were done as described for FptX. The supernatant was loaded
126 onto a 1-mL StrepTrap HP column (GE Healthcare) equilibrated with buffer A (50 mM Tris-HCl pH 8,
127 50 mM NaCl, 0.1 % DDM). The FadD1-FptX complex was eluted in buffer A supplemented with 2.5 mM
128 D-Desthiobiotin (Sigma Aldrich) into a 1-mL HisTrap HP column (GE Healthcare). The column was
129 washed in buffer A and the FadD1-FptX complex was eluted in buffer A supplemented with 250 mM

130 imidazole. Central fraction of the peak was then loaded onto a Superdex 200 column 10/300 GL (GE
131 Healthcare) equilibrated with 50 mM Tris-HCl pH 8, 50 mM NaCl, 0.025 % DDM. The FadD1-FptX
132 complex was eluted as a single peak, and the central fraction was immediately used for EM sample
133 preparation.

134

135 **EM processing of FptX, FadD1 and the FadD1-FptX complex.**

136 Determination of FadD1-FptX complex, FptX and FadD1 proteins structure was made by negative-stain
137 EM. 5 μL of FadD1-FptX complex ($28 \text{ ng}\cdot\mu\text{L}^{-1}$), FptX ($23 \text{ ng}\cdot\mu\text{L}^{-1}$) and FadD1 ($6.25 \text{ ng}\cdot\mu\text{L}^{-1}$) sample was
138 fixed with 0.6 μL glutaraldehyde 1%. The sample was then spotted to 300 meshes Cu grids covered with a
139 carbon film (Euromedex CF300-CU-050). After 60s of absorption, each sample was stained with 2% uranyl
140 acetate. For the FadD1-FptX complex, the sample was washed with one drop of 50 mM Tris pH 8, 50 mM
141 NaCl before staining with 2% uranyl acetate. Images were recorded automatically using the SerialEM
142 software on a FEI Tecnai F20 microscope operating at a voltage of 200 kV and a defocus range of 500 nm,
143 using a Gatan US1000 detector at a nominal magnification of 50,000X, yielding a pixel size of 2.12. A dose
144 rate of 20 electrons per square angstrom per second, and an exposure time of 10s were used. For the FadD1-
145 FptX complex, a total of 58,034 particles were selected from 3,000 independent images and extracted within
146 boxes of 200 pixels using Relion2. For FptX, a total of 38,746 particles were selected from 1,500
147 independent images and extracted within boxes of 192 pixels using Relion2. For FadD1, a total of 102,978
148 particles were selected from 1,500 independent images and extracted within boxes of 120 pixels using
149 Relion2. The defocus value was estimated, and the contrast transfer function was corrected using CTF
150 estimation in Relion2. We used two rounds of reference-free 2D class averaging to clean up the selected
151 data set. High-populated classes displaying high-resolution features were conserved during the procedure
152 with a final data set of 30,355 particles for the FadD1-FptX complex, 33,001 particles for FptX and 61,553
153 particles for FadD1. An initial 3D model was generated in EMAN2. Relion2 auto-refine procedure was used
154 to obtain a final reconstruction at 33-Å, 26-Å and 17-Å resolution for FadD1-FptX, FptX and FadD1,
155 respectively, after masking and without symmetry constraints. Resolutions are based on the “gold standard”

156 Fourier shell correlation (FSC) (Fig. S4). USCF Chimera was used to display three-dimensional
157 reconstructions.

158

159 **Iron uptake assays and cell fractionation.**

160 Cells were cultured overnight in LB medium at 30°C, and afterwards at 30°C overnight in CAA medium.
161 Then, they were diluted in fresh CAA medium and grown at 30°C overnight. Bacteria were washed with
162 50 mM Tris-HCl at pH 8 and diluted to an OD_{600nm} of 1. The PCH-⁵⁵Fe complex was prepared as previously
163 described [22]. Cells were incubated 30 min with 200 nM PCH-⁵⁵Fe at 30°C. After incubation, cells were
164 centrifuged for 8 min at 6, 700 g to obtain the supernatant as the extracellular medium, and the cell pellet
165 which was resuspend in Tris-sucrose EDTA (Tris-HCl 0.2 M pH 8, EDTA 1 mM, sucrose 20 %).
166 Spheroplasts were obtained by adding 200 µg.mL⁻¹ lysozyme (Euromedex) to the suspension and incubated
167 at 4°C for 1 h. The suspension was centrifuged for 8 min at 6,700 g at 4°C to obtain the spheroplast pellet
168 and the periplasmic fraction (supernatant). The supernatant was ultracentrifuged (120, 000 g, 40 min, 4°C)
169 to clarify the periplasmic fraction. Spheroplast pellet was washed with Tris-HCl 0.2 M pH 8, sucrose 20 %,
170 and resuspend in cold water by vortexing. The suspension was then incubated with benzonase for
171 1 h at 37°C. The cytoplasmic fraction was isolated by ultracentrifugation (120,000 g, 40 min, 4°C). Pellet
172 was washed twice with cold water and resuspended in Tris-HCl 0.2 M pH 8, sucrose 20 % to obtain the
173 bacterial membranes.

174

175 **Deletion mutant construction.**

176 For the deletion of both *fadD1* and *fadD2* genes, PCR was used to generate a 500 bp DNA fragment
177 upstream of *fadD2* and a 500 bp DNA fragment downstream of *fadD1*, by using the primer pairs 1280/1281
178 and 1282/1151, respectively. Each PCR product was linked by overlapping PCR and products were digested
179 with HindIII and EcoRI and cloned into the suicide vector pEXG2, yielding pEXG2Δ*fadD1*Δ*fadD2*.
180 Deletion in the chromosomal genome of *P. aeruginosa* was generated by transferring the suicide vector
181 from *E. coli* SM10 strains into recipient strains allowing the plasmid to integrate into the chromosome, with

182 selection for gentamicin resistance. A second crossing-over event excising the vector was selected using
183 NaCl-free LB plates supplemented with 5 % sucrose. Deletions were confirmed by sequencing using
184 external primers.

185

186 **PCH production.**

187 Cells were cultured overnight in LB medium at 37°C, and afterwards at 30°C overnight in iron-deficient
188 CAA medium. They were then diluted to 0.1 OD_{600nm} units in fresh CAA medium and incubated at 30°C for
189 16 h. The extracellular medium was separated from the cells by centrifugation at 7,700 g for 15 min. The
190 pH of the supernatant was acidified by adding 1 M citric acid and PCH was extracted with dichloromethane.
191 Pyochelin concentration was determined by measuring the absorbance at 320 nm ($\epsilon = 4,300 \text{ L}\cdot\text{mol}^{-1}\cdot\text{cm}^{-1}$).
192 Results are expressed as a function of PCH produced (μM) to bacterial growth (OD_{600nm}).

193

194 **Significance tests**

195 Student's *t* test was used for two-group comparisons using unpaired two-tailed *t* test. Analyses were
196 performed using GraphPad Prism 8.

197

198 **Results**

199

200 **Identification of FptX interacting partners.** FptX is proposed as the inner membrane protein involved in
201 ferri-PCH uptake in *P. aeruginosa* [13-15]. In order to find other proteins involved in this pathway, we
202 looked for FptX-interacting partners by using a bacterial two-hybrid genome wide screening. The pKNT25-
203 fptX bait plasmid was combined with the *P. aeruginosa* PAO1 fragment prey libraries constructed in the
204 pUT18 vector by Houot *et al.*, 2012 [20]. Blue colonies reflecting a protein interaction with FptX were
205 identified, and the DNA sequence inserts contained in the pUT18 derivative vectors were further sequenced.
206 The prey fragments corresponded either to the 253 first amino acids of the fatty acid coenzyme-A ligase
207 FadD1, or to the 120 first amino acids of PA1316, a putative major facilitator superfamily transporter. Only

208 FadD1 was identified multiple times throughout this screen and the interaction between FadD1 and FptX
209 was validated by cloning the entire proteins in two-hybrid vectors (Fig. 1A). The interaction was also
210 confirmed by co-expressing FadD1 with a StrepII tag and FptX with a His₆ tag at the carboxy terminus in
211 *E. coli*. Total membranes were isolated and solubilized using the detergent DDM. The complex was
212 specifically isolated by a two-step affinity chromatography and the presence of FadD1(StrepII) (63 kDa)
213 and FptX(His₆) (44 kDa) was confirmed by immunoblot analysis (Fig. 1B and C). **Negative control with the**
214 **individual FptX(His₆) protein excluded any unspecific binding (Fig. S1).** The overall FptX(His₆) distribution
215 on SDS-PAGE reveals several bands ranging from 44 to 150 kDa, suggesting multimerization of the protein.
216 Altogether, these results revealed a new complex between the inner membrane transporter FptX and the
217 fatty acid coenzyme-A ligase FadD1.

218
219 **FadD1 is involved in PCH production rather than ferri-PCH uptake.** This interaction between FptX
220 and FadD1 must involve a biological role for FadD1 in the PCH pathway. Based on the role of FptX in ferri-
221 PCH uptake [15], we first investigated the possible involvement of FadD1 in iron uptake *via* PCH.
222 *P. aeruginosa* has in its genome two genes encoding closely related enzymes for the fatty acid metabolism,
223 FadD1 and FadD2, which exhibit 60 % identity [23]. We deleted the two *fadD* genes to avoid any functional
224 redundancy. PCH-⁵⁵Fe uptake assays were performed using a *P. aeruginosa* strain unable to produce PVD
225 and PCH ($\Delta pvdF\Delta pchA$) in order to control the PCH concentration and to have no iron uptake by PVD, the
226 other siderophore produced by *P. aeruginosa*. Cells were grown under iron-restricted conditions, harvested
227 and incubated in the presence of 200 nM PCH-⁵⁵Fe. After 30 min incubation, cells were pelleted and the
228 cytoplasmic, periplasmic and membrane fractions isolated by cell fractionation and the radioactivity
229 monitored in each cell compartment (Fig. 2).

230 In the $\Delta pvdF\Delta pchA$ control strain, most of the radioactivity (53 %) was found in the cytoplasm, 8 % in the
231 periplasm, 18 % associated to the membranes and 21 % still in the extracellular medium (Fig. 2), while for
232 the $\Delta fptX$ mutant most of ⁵⁵Fe was not imported into the bacteria and found in the extracellular medium
233 (Fig. 2). In the absence of FptX, the ferri-PCH complex cannot enter the cells, which is related to previous

234 data showing that the expression of *fptA*, encoding for the outer membrane transporter, is drastically
235 decreased in an $\Delta fptX$ mutant [24]. Regarding the $\Delta fadD1D2$ mutant, a very similar ^{55}Fe repartition was
236 observed compare to the control strain, indicating that FadD1 plays no role in iron acquisition by PCH.
237 We next investigated the effect of *fadD1D2* mutations on PCH production. WT and the corresponding
238 mutant strains were grown under iron-starvation conditions and PCH was extracted from growth medium
239 and its concentration determined using its characteristic absorbance at 320 nm. A 1.4-, 2.4-, and 4.4-fold
240 decrease in PCH concentration in the growth medium was observed for the $\Delta fadD1D2$, $\Delta fptX$ and
241 $\Delta fptX\Delta fadD1D2$ mutants respectively, compared to the wild type PAO1 strain (Fig. 3), suggesting a role of
242 FadD1 in PCH production and/or secretion.

243

244 **Biochemical and architectural analysis of FptX, FadD1 and the FadD1-FptX complex.**

245 In contrast to the available X-ray structure of the outer membrane transporter FptA [11], structural data are
246 still lacking for the inner membrane transporter FptX. The determination of the 3D structure of this polytopic
247 inner membrane protein remains very challenging because of the low expression levels of FptX even in
248 overproducing bacterial systems. Consequently, we then investigated the architecture of FptX, FadD1 and
249 the FadD1-FptX complex by negative-stain EM. First, the proteins were produced and purified from *E. coli*
250 membranes and their functional integrity was established by assessing the binding activity to ferri-PCH for
251 FptX and the FadD1-FptX complex, and the fatty acid coenzyme-A ligase activity for FadD1 (Fig. S2). EM
252 data set were collected, and reference-free two-dimensional class revealed characteristic views of the
253 FadD1-FptX complex, FptX and FadD1 (Fig. S3). The EM data set was used to reconstruct a 33-Å, 26-Å
254 and 17-Å resolution three-dimensional (3D) model of the FadD1-FptX complex, FptX and FadD1 proteins,
255 respectively (Fig. 4). FadD1-FptX complex is ~230 Å in height and ~150 Å in diameter. FptX is ~225 Å in
256 height and ~120 Å in diameter, and FadD1 is ~115 Å in height and ~90 Å in diameter. The FptX EM model
257 was then docked into the EM volume of the FadD1-FptX complex, showing that FptX occupies most of the
258 EM envelope of the complex (Fig. 4). However, at this low resolution and according to the small volume of

259 FadD1, the electron density may not have sufficiently distinctive features for an unambiguous placement of
260 FadD1 in the EM volume complex.

261

262 **Discussion**

263 The data presented here give new insights in the *P. aeruginosa* PCH siderophore pathway. Previous studies
264 had shown that FptA and FptX are the outer and inner membrane transporters involved in iron uptake by
265 the siderophore PCH [10-15]. Both proteins also play a role in PCH production: in $\Delta fptA$ and $\Delta fptX$ mutants
266 no more PCH-Fe is transported into bacteria, affecting the PCH-mediated signaling cascade, and hence PCH
267 production [14,24].

268 Here, the bacterial two-hybrid screen represented a powerful tool as it identified for the first time a fatty
269 acid coenzyme-A ligase enzyme, FadD1, as an interacting partner of the inner membrane transporter FptX.
270 FadD1 is described as a fatty acid coenzyme-A ligase involved in fatty acid metabolism in *P. aeruginosa*
271 [23]. To assess the physiological significance of the FadD1-FptX complex, we explored the impact of FadD1
272 on both ferri-PCH uptake and PCH production. We showed that FadD1 has no impact on iron uptake by
273 PCH but is required for optimum PCH production. FadD1 may play a role in biosynthesis and/or secretion
274 of PCH, but the data do not allow to discriminate between these two biological processes. Our findings
275 suggest a potential acylation of PCH. FadD1 might load a fatty acid chain to PCH, allowing PCH to be
276 anchored to the inner membrane during its synthesis as described previously for PVD, ferrichrome or
277 mycobactin [25-27]. For mycobactin, the fatty acid ligase FadD33 (also known as MbtM) was reported to
278 transfer a lipophilic aliphatic chain to the ϵ -amino group of the lysine mycobactin core [27]. In the case of
279 PVD, the biosynthesis begins with an acylation introducing a myristic or myristoleic group carried out by
280 the first module of the PvdL non-ribosomal peptide synthetase [26]. The presence of a myristic or
281 myristoleic acid group retains the PVD precursor at the membrane during its biosynthesis. For both PVD
282 and mycobactin, the acylation of siderophore promotes plasma membrane localization. **As FptX is involved**
283 **in ferri-PCH uptake, we can also hypothesize that such acylation of PCH could occur after its uptake for its**
284 **recovery/recycling, if any.**

285 Further experiments are still necessary to identify the role of an acylation of PCH by FadD1. Moreover,
286 currently nothing is known concerning the proteins and the molecular mechanisms involved in PCH
287 secretion as well as in the molecular mechanism allowing iron release from PCH.
288 FptX was reported to be a homolog of the transporter of rhizobactin RhtX, belonging to the major facilitator
289 superfamily (MFS) transporters [13]. Currently, structure determination of such inner membrane proteins
290 remains a difficult task and presents a challenge for expression and purification. Here, we established for
291 the first time a low-resolution 3D model of FptX, its interacting partner FadD1 and of the FadD1-FptX
292 complex by negative-stain EM. Due to the lack of information concerning the various domains of FptX and
293 the low resolution of the EM reconstruction, it was impossible to clearly define a topology of the complex.
294 Altogether, these results highlight a new actor in the PCH pathway and suggest that this pathway would
295 probably be more complex than what has been described so far. In addition, our efforts to purify and initiate
296 low resolution EM-models pave the way for future high-resolution studies for structure-based drug design
297 to counter antibiotic resistance, one of the biggest public health challenges of our time.

298

299 **Acknowledgement**

300 Authors acknowledge the Centre National de la Recherche Scientifique (CNRS) for general financial
301 support. BR would like to thank Roche Pharmaceutical Research and Early Development Basel for their
302 financial support via the Roche Postdoctoral Fellowship (RPF) Program. We acknowledge the support and
303 the use of resources of the French Infrastructure for Integrated Structural Biology (FRISBI) ANR-10-INBS-
304 05, “Project ID 52”, and of Instruct-ERIC, “PID 2886”. Specifically, we would like to thank Christine
305 Ruhlmann and Corinne Crucifix (IGBMC, Strasbourg) for help with EM sample preparation and EM data
306 collection, and Veronique Mallouh (IGBMC, Strasbourg) for help with data processing. We acknowledge
307 Eric Durand (LISM, Marseille) for fruitful EM processing discussion. We acknowledge Christophe Bordi
308 (LISM, Marseille), Laetitia Houot (LISM, Marseille) and Aurélia Battesti (LCB, Marseille) for kindly
309 providing the PAO1 two-hybrid libraries and the two-hybrid vectors, and Laurent Loiseau (LCB, Marseille)
310 for providing pBAD vectors.

311 Author contributions

312 BR and IS designed the experiments. BR performed the experiments. GM provided the PCH siderophore.
313 BR wrote the manuscript. IS helped to improve the article. All authors discussed and commented on the
314 manuscript.

315

316 References

317 1 Tommasi R, Brown DG, Walkup GK, Manchester JI & Miller AA (2015) ESKAPEing the labyrinth of
318 antibacterial discovery. *Nat Rev Drug Discov* **14**, 529–542.

319 2 Cox CD, Rinehart KL, Moore ML & Cook JC (1981) Pyochelin: novel structure of an iron-chelating
320 growth promoter for *Pseudomonas aeruginosa*. *Proc Natl Acad Sci U S A* **78**, 4256–4260.

321 3 Thomas MS (2007) Iron acquisition mechanisms of the Burkholderia cepacia complex. *Biometals Int J*
322 *Role Met Ions Biol Biochem Med* **20**, 431–452.

323 4 Schalk IJ (2018) Siderophore-antibiotic conjugates: exploiting iron uptake to deliver drugs into bacteria.
324 *Clin Microbiol Infect Off Publ Eur Soc Clin Microbiol Infect Dis* **24**, 801–802.

325 5 Hider RC & Kong X (2010) Chemistry and biology of siderophores. *Nat Prod Rep* **27**, 637–657.

326 6 Hare NJ, Soe CZ, Rose B, Harbour C, Codd R, Manos J & Cordwell SJ (2012) Proteomics of
327 *Pseudomonas aeruginosa* Australian epidemic strain 1 (AES-1) cultured under conditions mimicking the
328 cystic fibrosis lung reveals increased iron acquisition via the siderophore pyochelin. *J Proteome Res* **11**,
329 776–795.

330 7 Rossi E, Falcone M, Molin S & Johansen HK (2018) High-resolution in situ transcriptomics of
331 *Pseudomonas aeruginosa* unveils genotype independent patho-phenotypes in cystic fibrosis lungs. *Nat*
332 *Commun* **9**, 3459.

333 8 Lyczak JB, Cannon CL & Pier GB (2002) Lung infections associated with cystic fibrosis. *Clin*
334 *Microbiol Rev* **15**, 194–222.

335 9 Reimmann C, Serino L, Beyeler M & Haas D (1998) Dihydroaeruginoinic acid synthetase and pyochelin
336 synthetase, products of the pchEF genes, are induced by extracellular pyochelin in *Pseudomonas*

- 337 aeruginosa. *Microbiol Read Engl* **144** (Pt 11), 3135–3148.
- 338 10 Ankenbauer RG (1992) Cloning of the outer membrane high-affinity Fe(III)-pyochelin receptor of
339 *Pseudomonas aeruginosa*. *J Bacteriol* **174**, 4401–4409.
- 340 11 Cobessi D, Celia H & Pattus F (2005) Crystal structure at high resolution of ferric-pyochelin and its
341 membrane receptor FptA from *Pseudomonas aeruginosa*. *J Mol Biol* **352**, 893–904.
- 342 12 Mislin GLA, Hoegy F, Cobessi D, Poole K, Rognan D & Schalk IJ (2006) Binding properties of
343 pyochelin and structurally related molecules to FptA of *Pseudomonas aeruginosa*. *J Mol Biol* **357**, 1437–
344 1448.
- 345 13 Cuív PO, Clarke P, Lynch D & O’Connell M (2004) Identification of *rhtX* and *fptX*, novel genes
346 encoding proteins that show homology and function in the utilization of the siderophores rhizobactin 1021
347 by *Sinorhizobium meliloti* and pyochelin by *Pseudomonas aeruginosa*, respectively. *J Bacteriol* **186**,
348 2996–3005.
- 349 14 Michel L, Bachelard A & Reimann C (2007) Ferripyochelin uptake genes are involved in pyochelin-
350 mediated signalling in *Pseudomonas aeruginosa*. *Microbiol Read Engl* **153**, 1508–1518.
- 351 15 Cunrath O, Gasser V, Hoegy F, Reimann C, Guillon L & Schalk IJ (2015) A cell biological view of
352 the siderophore pyochelin iron uptake pathway in *Pseudomonas aeruginosa*. *Environ Microbiol* **17**, 171–
353 185.
- 354 16 Noël S, Gasser V, Pesset B, Hoegy F, Rognan D, Schalk IJ & Mislin GLA (2011) Synthesis and
355 biological properties of conjugates between fluoroquinolones and a N3’’-functionalized pyochelin. *Org*
356 *Biomol Chem* **9**, 8288–8300.
- 357 17 Paulen A, Hoegy F, Roche B, Schalk IJ & Mislin GLA (2017) Synthesis of conjugates between
358 oxazolidinone antibiotics and a pyochelin analogue. *Bioorg Med Chem Lett* **27**, 4867–4870.
- 359 18 Ghosh M, Miller PA, Möllmann U, Claypool WD, Schroeder VA, Wolter WR, Suckow M, Yu H, Li S,
360 Huang W, Zajicek J & Miller MJ (2017) Targeted Antibiotic Delivery: Selective Siderophore Conjugation
361 with Daptomycin Confers Potent Activity against Multidrug Resistant *Acinetobacter baumannii* Both in
362 Vitro and in Vivo. *J Med Chem* **60**, 4577–4583.

- 363 19 Liu R, Miller PA, Vakulenko SB, Stewart NK, Boggess WC & Miller MJ (2018) A Synthetic Dual
364 Drug Sideromycin Induces Gram-Negative Bacteria To Commit Suicide with a Gram-Positive Antibiotic.
365 *J Med Chem* **61**, 3845–3854.
- 366 20 Houot L, Fanni A, de Bentzmann S & Bordi C (2012) A bacterial two-hybrid genome fragment library
367 for deciphering regulatory networks of the opportunistic pathogen *Pseudomonas aeruginosa*. *Microbiol*
368 *Read Engl* **158**, 1964–1971.
- 369 21 Battesti A & Bouveret E (2012) The bacterial two-hybrid system based on adenylate cyclase
370 reconstitution in *Escherichia coli*. *Methods San Diego Calif* **58**, 325–334.
- 371 22 Gasser V, Baco E, Cunrath O, August PS, Perraud Q, Zill N, Schleberger C, Schmidt A, Paulen A,
372 Bumann D, Mislin GLA & Schalk IJ (2016) Catechol siderophores repress the pyochelin pathway and
373 activate the enterobactin pathway in *Pseudomonas aeruginosa*: an opportunity for siderophore-antibiotic
374 conjugates development. *Environ Microbiol* **18**, 819–832.
- 375 23 Kang Y, Zarzycki-Siek J, Walton CB, Norris MH & Hoang TT (2010) Multiple FadD acyl-CoA
376 synthetases contribute to differential fatty acid degradation and virulence in *Pseudomonas aeruginosa*.
377 *PloS One* **5**, e13557.
- 378 24 Michel L, González N, Jagdeep S, Nguyen-Ngoc T & Reimann C (2005) PchR-box recognition by
379 the AraC-type regulator PchR of *Pseudomonas aeruginosa* requires the siderophore pyochelin as an
380 effector. *Mol Microbiol* **58**, 495–509.
- 381 25 Hannauer M, Barda Y, Mislin GLA, Shanzer A & Schalk IJ (2010) The ferrichrome uptake pathway in
382 *Pseudomonas aeruginosa* involves an iron release mechanism with acylation of the siderophore and
383 recycling of the modified desferrichrome. *J Bacteriol* **192**, 1212–1220.
- 384 26 Hannauer M, Schäfer M, Hoegy F, Gizzi P, Wehrung P, Mislin GLA, Budzikiewicz H & Schalk IJ
385 (2012) Biosynthesis of the pyoverdine siderophore of *Pseudomonas aeruginosa* involves precursors with a
386 myristic or a myristoleic acid chain. *FEBS Lett* **586**, 96–101.
- 387 27 Vergnolle O, Xu H & Blanchard JS (2013) Mechanism and regulation of mycobactin fatty acyl-AMP
388 ligase FadD33. *J Biol Chem* **288**, 28116–28125.

389 28 Vincent F, Round A, Reynaud A, Bordi C, Filloux A & Bourne Y (2010) Distinct oligomeric forms of
390 the *Pseudomonas aeruginosa* RetS sensor domain modulate accessibility to the ligand binding site.
391 *Environ Microbiol* **12**, 1775–1786.

392

393 **Figure legends**

394

395 **Fig. 1.** Interaction between FptX and FadD1. (A) Bacterial two-hybrid assay. The *fadD1* and *fptX* genes
396 were cloned into the two-hybrid pUT18C or pKNT25 vectors and corresponding vectors were co-
397 transformed in DHM1 cells that were spotted on Xgal-IPTG LB agar plates. A blue color reflects interaction
398 between chimeric proteins while white color attests the absence of interaction. RetS was reported to form
399 dimers and is used as a positive control [28]. The experiments were done in triplicate and a representative
400 result is shown. (B) Two-step affinity chromatography. Solubilized bacterial membranes overexpressing
401 FadD1(StrepII) and FptX(His₆) proteins were submitted to a two-step affinity chromatography: loading into
402 a StrepTrap HP column (1), elution with desthiobiotin into a HisTrap HP column (2), and final elution with
403 imidazole (3) **as described in the Materials and Methods section**. (C) Immunoblot analysis of the fractions
404 corresponding to the different chromatography steps using anti-His (α -His) and anti-StrepII (α -StrepII)
405 antibodies.

406

407 **Fig. 2.** ⁵⁵Fe distribution in *P. aeruginosa* cell compartments after incubation with PCH-⁵⁵Fe. Strains were
408 grown in CAA medium and then incubated in the presence of 200 nM PCH-⁵⁵Fe during 30 min. Afterwards,
409 the cells were then pelleted; the extracellular medium, periplasm, cytoplasm and membrane fractions
410 isolated as described in the Materials and methods, and the amount of ⁵⁵Fe present monitored. The results
411 are expressed as the percentage of pmol of ⁵⁵Fe incubated with the cells. The errors bars represent the
412 standard deviation of the mean of three independent experiments.

413 **Fig. 3.** Amount of PCH secreted by PAO1 and its corresponding mutants. Cells were grown in CAA medium
414 and PCH was extracted from the growth medium as described in Materials and Methods and its

415 concentration was determined by measuring the absorbance at 320 nm. The errors bars represent the
416 standard deviation of the mean of six independent experiments. Student's t-tests were performed between
417 data (****P < 0.0001).

418

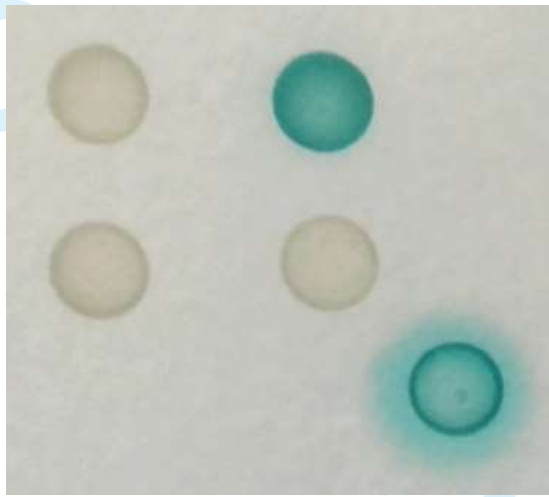
419 **Fig. 4.** Architecture of the purified proteins. 33-Å 3D reconstruction of the FadD1-FptX complex (A), 26-
420 Å 3D reconstruction of FptX (B) and 17-Å 3D reconstruction of FadD1(C) without symmetry applied. The
421 maps are displayed in different views. (D) Fitting of FptX (orange) in the EM volume of the FadD1-FptX
422 complex (grey) without symmetry applied.

423

For Review Only

A

T18

FadD1
-
RetS

T25

FEBS Letters

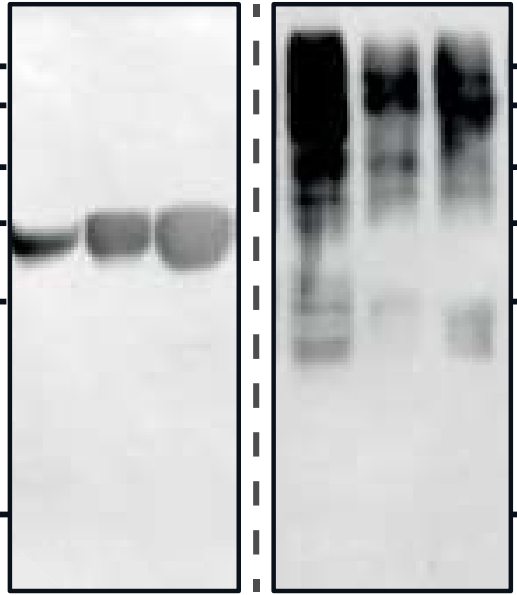
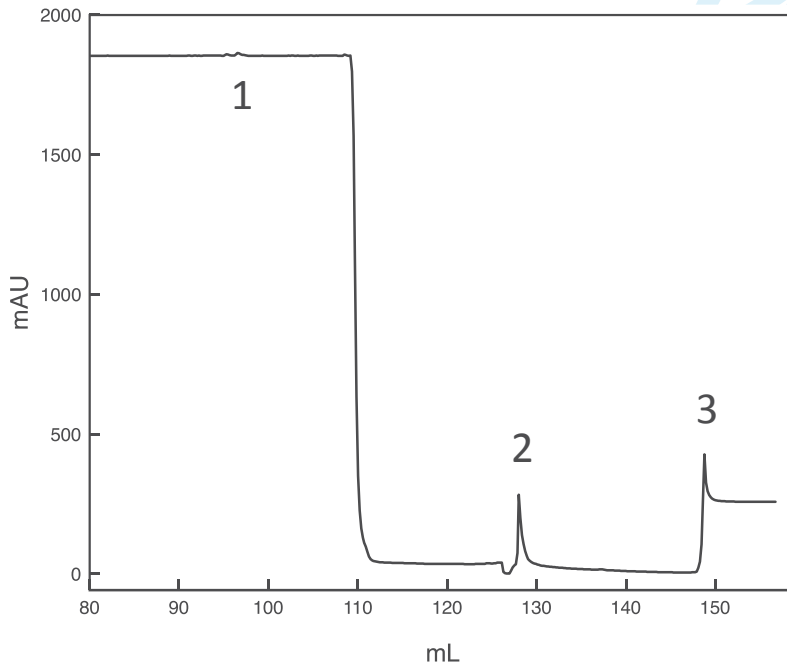
FptX RetS

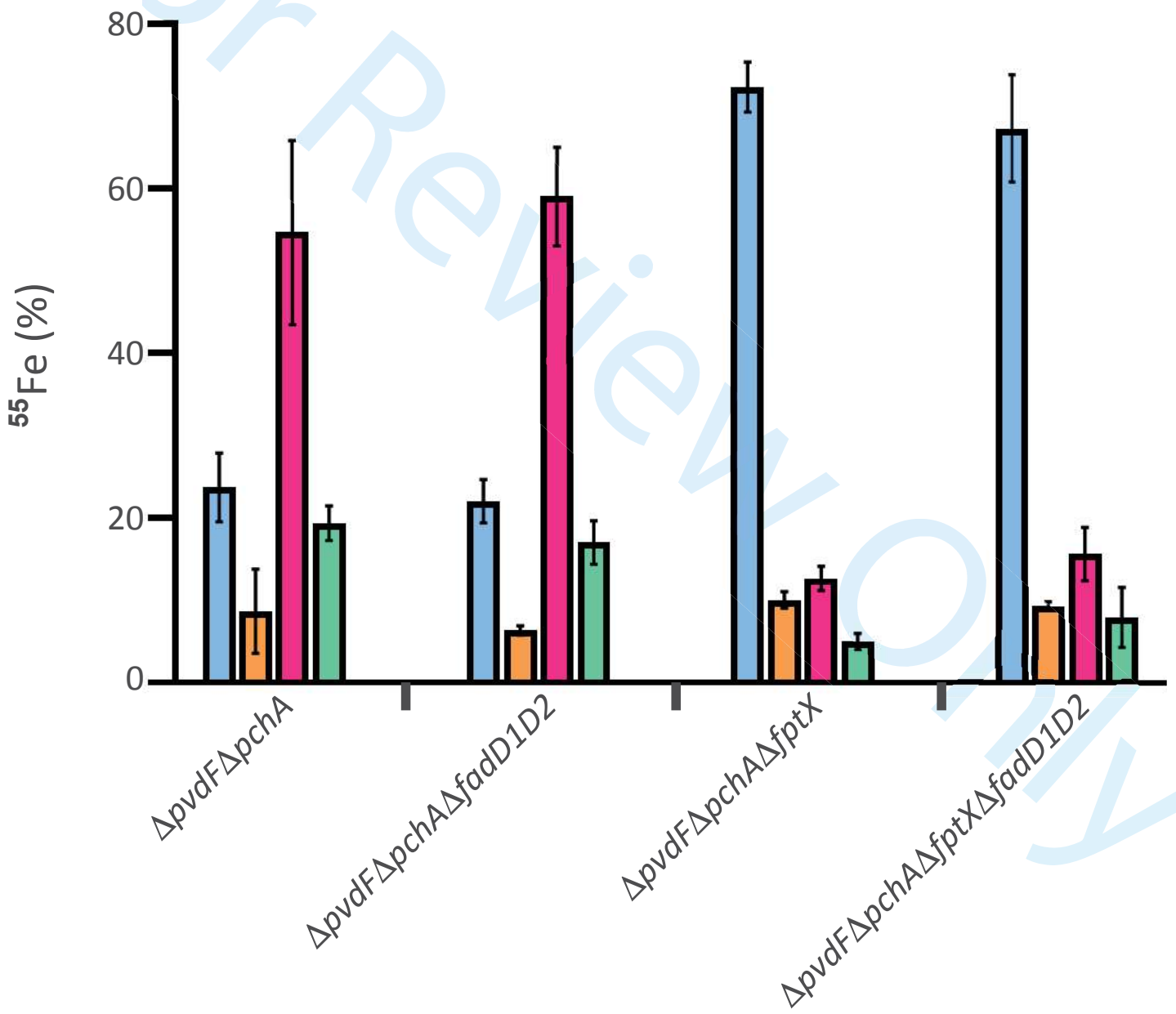
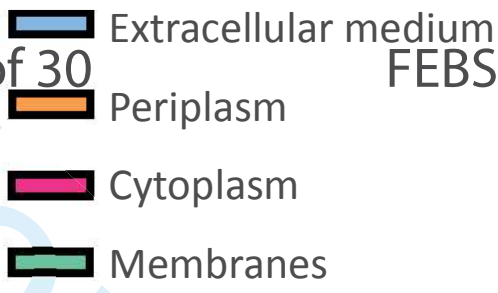
C α -Strep

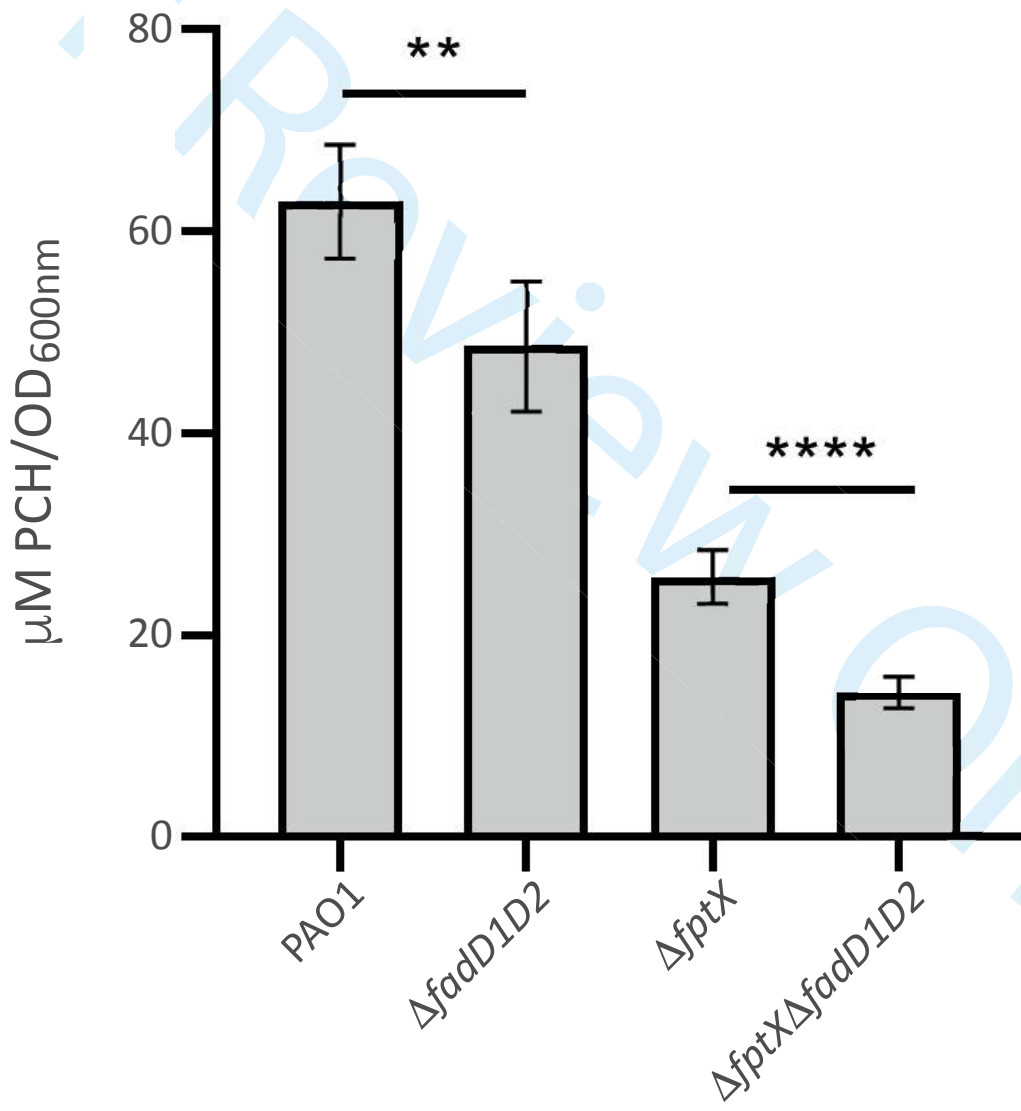
Page 18 of 30

1 2 3

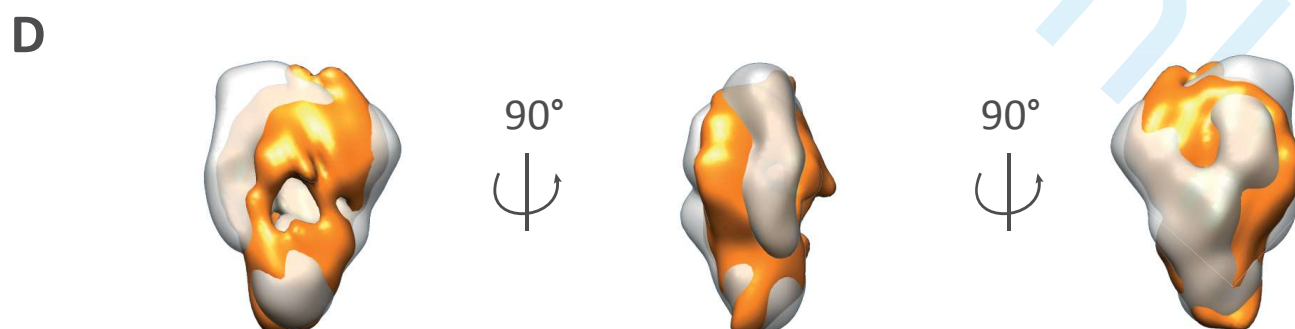
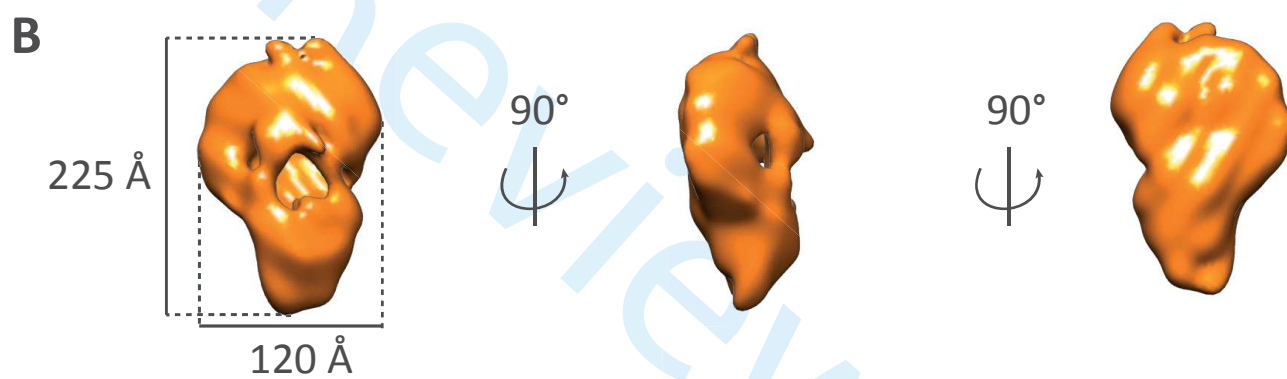
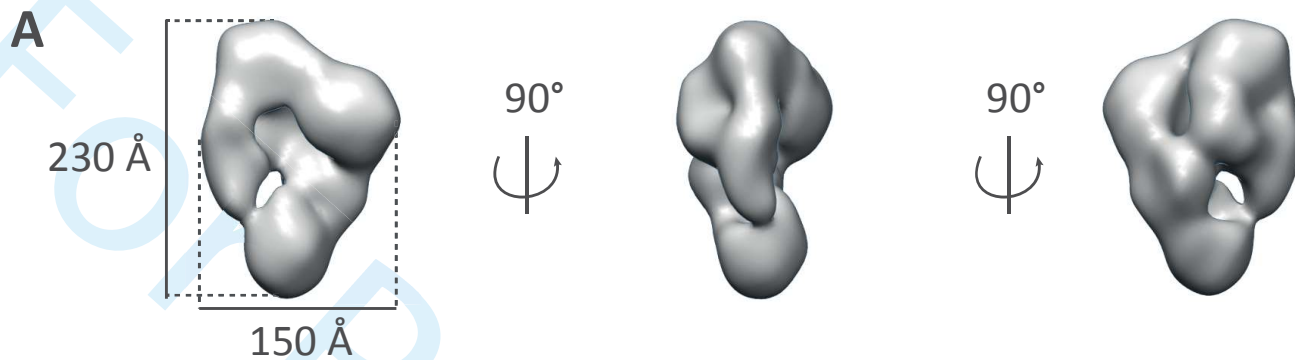
1 2 3

250
130
100
70
55
35250
130
100
70
55
35**B**





FEBS Letters



Supplementary data

1

2

3 **Identification of the fatty acid coenzyme-A ligase FadD1 as an interacting partner of FptX in the** 4 ***Pseudomonas aeruginosa* pyochelin pathway**

5

6 Béatrice Roche^{1,2,3*}, Gaëtan L.A. Mislin^{1,2} and Isabelle J. Schalk^{1,2}7 ¹. CNRS, UMR7242, ESBS, Bld Sébastien Brant, F-67412 Illkirch, France.8 ². Université de Strasbourg, UMR7242, ESBS, Bld Sébastien Brant, F-67412 Illkirch, France.9 ³. Present address: Biozentrum, University of Basel, CH-4056 Basel, Switzerland

10 * = correspondence should be addressed to Béatrice Roche (beatrice.roche@unibas.ch)

11

12 **Materials and methods**

13

14 **Binding of PCH-⁵⁵Fe.**

15 10 nM of purified FptX or the complex was incubated with various amount of PCH-⁵⁵Fe in 500 µL of 50
16 mM Hepes pH 7.5, 50 mM NaCl, 0.025 % DDM at room temperature for 2 h. The solution of PCH
17 complexed with ⁵⁵Fe was prepared with a siderophore/iron (mol/mol) ratio of 20:1. Incubation was stopped
18 by filtering the assay mixture over GF/B filters (Whatman, presoaked in 0.1 % polyethyleneimine to reduce
19 the non-specific retention). The filters were then rapidly washed three times with 1 mL of 50 mM Tris pH
20 8 and counted for radioactivity in a scintillation mixture. The experiment was repeated in the absence of the
21 purified protein. For each PCH-⁵⁵Fe concentration, the non-specific retention was then subtracted from the
22 total radioactivity monitored in the presence of the protein.

23

24 **Measurement of fatty acyl-CoA synthetase activity of FadD1.**

25 The activity of purified FadD1 was assessed using Ellman's reagent to monitor the consumption of the free
26 thiol group of Co-A due to FadD1-catalyzed acyl-CoA ligation [1]. This colorimetric assay quantifies the

27 instantaneous free thiol concentration via absorbance readings at 412 nm. A color change is produced upon
28 the binding of 5,5'-dithiobis-(2-nitrobenzoic acid) (DTNB or Ellman's reagent) to the free thiol groups of
29 CoA-SH. Progressive loss of signal at 412 nm is indicative of CoA-SH consumption. Reactions were
30 prepared with 40 µg of purified FadD1 in a reaction buffer containing final concentrations of 150 mM Tris-
31 HCl (pH 7.2), 10 mM MgCl₂, 2 mM EDTA, 0.1 % Triton X-100, 5 mM ATP, 0.5 mM co-enzyme A and
32 sodium oleate (0 and 200 µM). To perform the reaction, each mixture was assembled containing all
33 components above (excluding CoASH). The reaction mixture was prewarmed at 37°C for 2 min. The
34 reaction was initiated with the addition of CoASH (final concentration 0.5 mM) that was pre-incubated at
35 37°C for 2 min, quickly mixed, and incubated at 37°C during the course of the reaction. 70 µL aliquots of
36 the reaction were taken at different intervals and mixed with 600 µL of 0.4 mM DTNB (dissolved in 0.1 M
37 potassium phosphate at pH 8). A_{412nm} values were acquired after a 5-minute color development period at
38 room temperature. Control reaction mixture lacking protein was also prepared. The previously published
39 extinction coefficient of 13,600 M⁻¹.cm⁻¹ for DTNB was used to compute specific activity [1].

40

41 **Loading of the individual FptX(His₆) into a StrepTrap HP column.**

42 Top10 *E. coli* cells were transformed with the p33-fptX(His₆) vector. Cell growth, gene induction and
43 membrane preparation were done as described in the "Expression and purification of FptX" section in the
44 main Materials and Methods. The supernatant was loaded onto a 1-mL StrepTrap HP column (GE
45 Healthcare) equilibrated with buffer A (50 mM Tris-HCl pH 8, 200 mM NaCl, 0.1 % DDM). Elution was
46 done using buffer A containing 2.5 mM D-Desthiobiotin. The unbound fraction was then loaded onto a
47 1-mL HisTrap HP column (GE Healthcare) equilibrated with buffer B (50 mM Tris-HCl pH 8, 500 mM
48 NaCl, 0.1 % n-Dodecyl-β-D-maltopyranoside (DDM), 20 mM imidazole). Elution was done with buffer B
49 containing 500 mM imidazole.

50

51

52

53 **Figure legends**

54
55 **Fig. S1.** Negative control by loading the individual FptX(His₆) onto the StrepTrap column. (A) Solubilized
56 bacterial membranes overexpressing FptX(His₆) only were loaded onto a StrepTrap HP column: Unbound
57 (U1) and elution with desthiobiotin steps are represented. (B) The unbound U1 fraction was then loaded
58 onto a HisTrap HP column and eluted with imidazole. (C) Immunoblot analysis of the different steps of this
59 procedure using anti-His (α -His) antibodies.

60
61 **Fig. S2.** Purification and biochemical characterization of FptX, FadD1 and the FadD1-FptX complex.
62 (A, D and G) Size-exclusion chromatography analysis of the purified FptX (A), FadD1 (D) and the FadD1-
63 FptX complex (G) (continuous line) on a Superdex 200 10/300 GL. The dead volume is indicated as the V₀.
64 The arrow indicates the position of the fraction corresponding to FptX (A), FadD1 (D) and the FadD1-FptX
65 complex (G). (B and H) Immunoblot analysis of the purified FptX (B) and the FadD1-FptX complex (H)
66 using anti-His (α -His) and anti-StrepII (α -Strep) antibodies. (C and I) Binding of PCH-⁵⁵Fe to purified FptX
67 (C) and FadD1-FptX complex (I). Purified proteins were incubated with 10, 100 or 200 nM of PCH-⁵⁵Fe
68 complex. The non-specific retention was subtracted from the total of radioactivity monitored in the presence
69 of the proteins. (E) SDS-PAGE of the purified FadD1 protein analyzed by Instant blue™ staining. (F) FadD1
70 enzymatic assay was conducted using DTNB to monitor CoA-SH consumption at 412 nm with increasing
71 amount of sodium oleate as substrate. A loss of signal at 412 nm is indicative of FadD1 activity. The errors
72 bars represent the standard deviation of the mean of three independent experiments.

73
74 **Fig. S3.** Representative electron micrograph showing FadD1-FptX (A), FptX (D) and FadD1 (G) particles
75 present in several orientations. Scale bar, (A and G) 50 nm, (D) 20nm. Representative views of FadD1-FptX
76 (B), FptX (E) and FadD1 (H). Typical class averages of FadD1-FptX (C), FptX (F) and FadD1 (I).

77

78 **Fig. S4.** FSC curves of FptX (A), the FadD1-FptX complex (B) and FadD1 (C) reconstruction without
 79 symmetry applied. The FSC curves were calculated in Relion using the masked reconstruction of FptX, the
 80 FadD1-FptX complex and FadD1, respectively.

81

82 **Table S1.** Strains and plasmids used in this study.

Strains	ID collection	Characteristics	Reference
<i>Escherichia coli</i>			
TOP10	2	F-, <i>mcrA</i> Δ (<i>mrr-hsdRMS-mcrBC</i>), ϕ 80 <i>lacZ</i> , Δ <i>M15</i> , Δ <i>lacX74</i> , <i>recA1</i> , <i>araD139</i> , Δ (<i>ara-leu</i>)7697, <i>galU</i> , <i>galK</i> , <i>rpsL</i> , <i>endA1</i> , <i>mup</i>	Invitrogen
<i>E. coli</i> DHM1	281	F-, <i>cya</i> -, <i>recA1</i> , <i>endA</i> , <i>gyrA96</i> , <i>thi-1</i> , <i>hsdR17</i> , <i>spoT1</i> , <i>rjbD1</i> , <i>cya-854</i>	[2]
<i>Pseudomonas aeruginosa</i>			
PAO1	43	Wild-type strain	[3]
<i>ΔfptX</i>	PAS218	PAO1; <i>fptX</i> chromosomally deleted	[4]
<i>ΔfadD1D2</i>	PAS431	PAO1; <i>fadD1</i> and <i>fadD2</i> chromosomally deleted	This study
<i>ΔfptX ΔfadD1D2</i>	PAS410	PAO1; <i>fadD1</i> , <i>fadD2</i> and <i>fptX</i> chromosomally deleted	This study
<i>ΔpvdFΔpchA</i>	PAS213	PAO1; <i>pvdF</i> and <i>pchA</i> chromosomally deleted	[4]
<i>ΔpvdFΔpchAΔfptX</i>	PAS273	PAO1; <i>pvdF</i> , <i>pchA</i> and <i>fptX</i> chromosomally deleted	[4]
<i>ΔpvdFΔpchAΔfadD1D2</i>	PAS428	PAO1; <i>pvdF</i> , <i>pchA</i> , <i>fadD1</i> and <i>fadD2</i> chromosomally deleted	This study
<i>ΔpvdFΔpchAΔfptXΔfadD1D2</i>	PAS413	PAO1; <i>pvdF</i> , <i>pchA</i> , <i>fptX</i> , <i>fadD1</i> and <i>fadD2</i> chromosomally deleted	This study
Plasmids	ID collection	Characteristics	Reference
pKNT25	264	P15 origin, Plac, C-terminal T25 cyclase fragment, Kan ^R	[2]
pUT18C	265	ColE1 origin, Plac, N-terminal T18 cyclase fragment, Ap ^R	[2]
pBAD33	270	pBAD33 plasmid, Cm ^R	[5]
pBAD24	271	pBAD24 plasmid, Ap ^R	[5]
pUT18CPAO1lib	294	pUT18C containing PAO1 genomic library as a C-terminal T18 fusion	[6]
pUT18PAO1lib	295	pUT18 containing PAO1 genomic library as an N-terminal T18 fusion	[6]
pUT18+1PAO1lib	296	pUT18+1 containing PAO1 genomic library as an N-terminal T18 fusion	[6]
pUT18+2PAO1lib	297	pUT18+2 containing PAO1 genomic library as an N-terminal T18 fusion	[6]
pKNT25-fptX	268	pKNT25 plasmid containing <i>fptX-cyaAT25</i> fusion	This study
pUT18C-fadD1	293	pUT18C plasmid containing <i>cyaAT18-fadD1</i> fusion	This study
p33-fptX(His ₆)	272	pBAD33 plasmid expressing <i>fptX</i> Cter-fused to 6His tag	This study
p24-fadD1(StrepII)	311	pBAD24 plasmid expressing <i>fadD1</i> Cter-fused to StrepII tag	This study
pEXG2 delfadD1D2	330	suicide vector for deleting <i>fadD1</i> and <i>fadD2</i>	This study

83

84

85

86

87

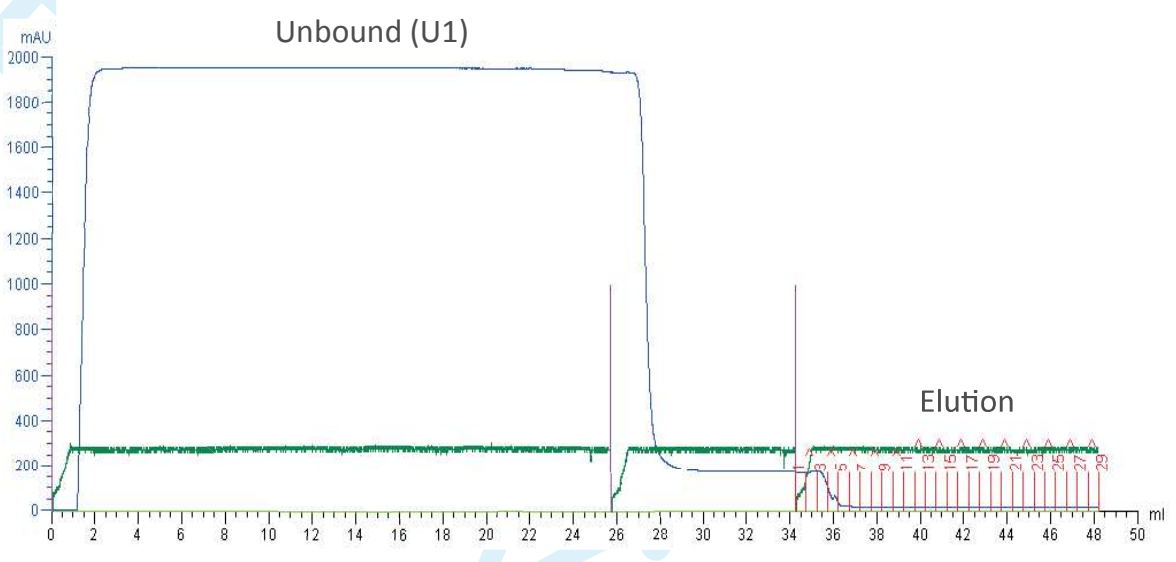
88

89 **Table S2.** Oligonucleotides used in this study.

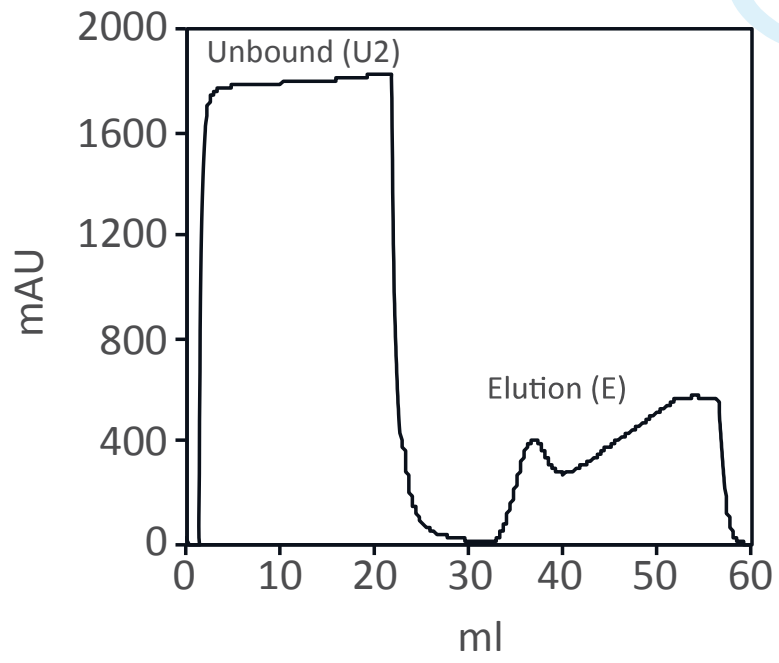
Name	ID collection	Sequence (5' → 3')
pKT25-fptXXbaI	951	CCGGTCTAGAGATGCTTGAGCTGTACCGCCACCGC
pKT25-fptXKpnI	952	CCGGGTACCTCAGGCCTTCCGCCCGCCCTT
pKT25-fadD1UP	1037	CCGGTCTAGAGATGATCGAAAACCTTCTGGAAGGAC
pKT25-fadD1DO	1038	CCGGGTACCCGCTTCTGGCCCGCTTCTTCAGCTC
fptX-UEcoRI	970	CCGGGAATTCAAGGAGATATACATATGCTTGAGCTGTACCGCCACCGC
fptX-DOHindIII	969	CCGGAAGCTTTTCAGGCCTTCCGCCCGCCCTT
fadD1-UPp24	1157	CCGGCCATGGCCATCGAAAACCTTCTGGAAGGACAAG
fadD1-DOSTrepCter	1158	CCGGAAGCTTTTCATTTTTTCGAACTGCGGGTGGCTCCAGCTAGCCTTCTGGCCCGCTTTC TTCAGCT
DelfadD1-500UPHindIII	1150	CCGGAAGCTTGCTTCAATGTCTACCCCAACGAGATCGAAG
DelfadD1-500DO EcoRI	1151	CCGGGAATTCGGGAAGGAGTCTGGTTCGGTCATCTAGGCTT
Del fadD1-ATG rev	1152	TGGTACTTGTCTTCCAGAAAGTTTTTCGATCAT
Del fadD1-STOP for	1153	TCTGGAAGGACAAGTACCCACTGCGCGACGAAGAGCTGAAGAAA
Del fadD2-500UPHindIII	1280	CCGGAAGCTTTTGCCTCCAGCCCTGGTTCGGCGAAGTGG
Del ATG-fadD2 rev	1281	TTCAAGTTGCATTTATTCTTGTCTCTTACCTG
Del STOP-fadD1fadD2 for	1282	GTAAGAGGACAAGAATAAATGCAACCTGAAAAAGCGGGCCAGAAGTAAGTCCGC

90

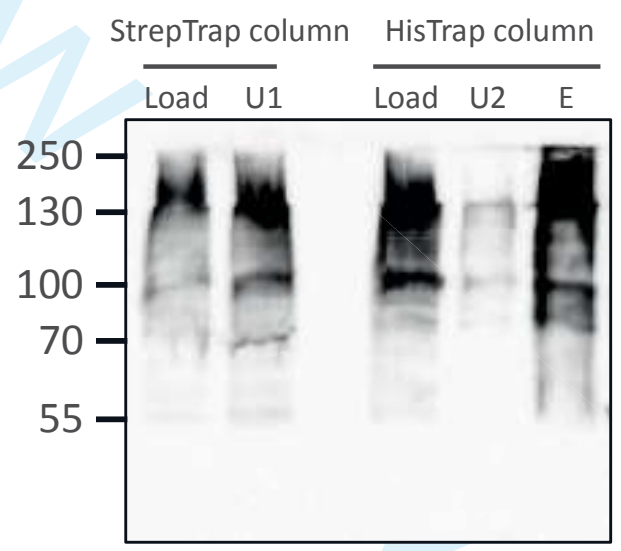
91 **References**92 1 Ellman GL (1959) Tissue sulfhydryl groups. *Arch Biochem Biophys* 82, 70–77.93 2 Karimova G, Dautin N & Ladant D (2005) Interaction network among Escherichia coli membrane proteins
94 involved in cell division as revealed by bacterial two-hybrid analysis. *J Bacteriol* 187, 2233–2243.95 3 Stover CK, Pham XQ, Erwin AL, Mizoguchi SD, Warrenner P, Hickey MJ, Brinkman FS, Hufnagle WO,
96 Kowalik DJ, Lagrou M, Garber RL, Goltry L, Tolentino E, Westbrook-Wadman S, Yuan Y, Brody LL,
97 Coulter SN, Folger KR, Kas A, Larbig K, Lim R, Smith K, Spencer D, Wong GK, Wu Z, Paulsen IT, Reizer
98 J, Saier MH, Hancock RE, Lory S & Olson MV (2000) Complete genome sequence of Pseudomonas
99 aeruginosa PAO1, an opportunistic pathogen. *Nature* 406, 959–964.100 4 Cunrath O, Gasser V, Hoegy F, Reimann C, Guillon L & Schalk IJ (2015) A cell biological view of the
101 siderophore pyochelin iron uptake pathway in Pseudomonas aeruginosa. *Environ Microbiol* 17, 171–185.102 5 Guzman LM, Belin D, Carson MJ & Beckwith J (1995) Tight regulation, modulation, and high-level
103 expression by vectors containing the arabinose PBAD promoter. *J Bacteriol* 177, 4121–4130.104 6 Houot L, Fanni A, de Bentzmann S & Bordi C (2012) A bacterial two-hybrid genome fragment library for
105 deciphering regulatory networks of the opportunistic pathogen Pseudomonas aeruginosa. *Microbiol Read*
106 *Engl* 158, 1964–1971.



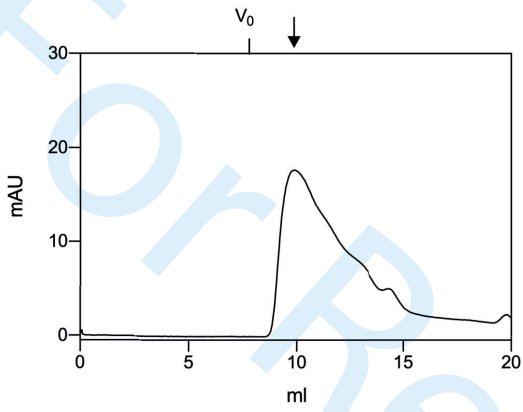
B



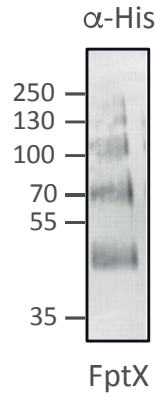
C



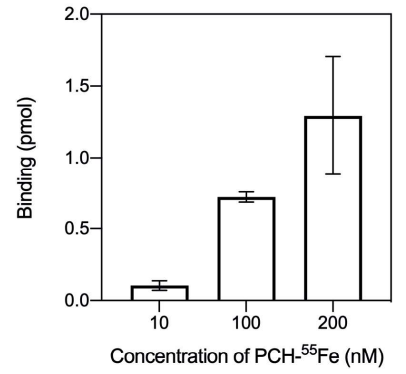
A



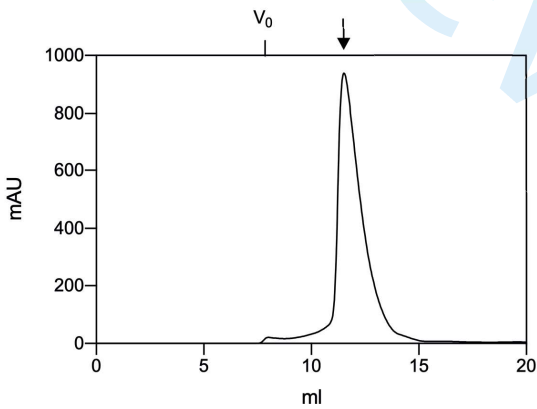
B



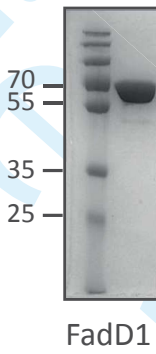
c



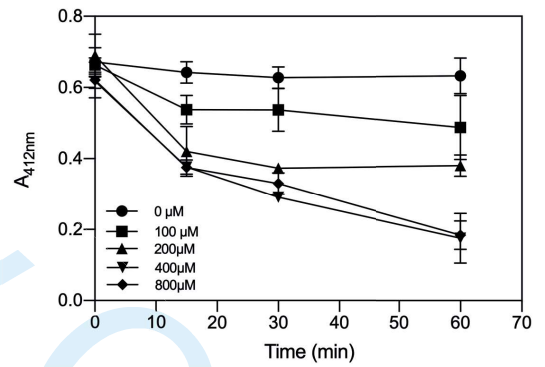
D



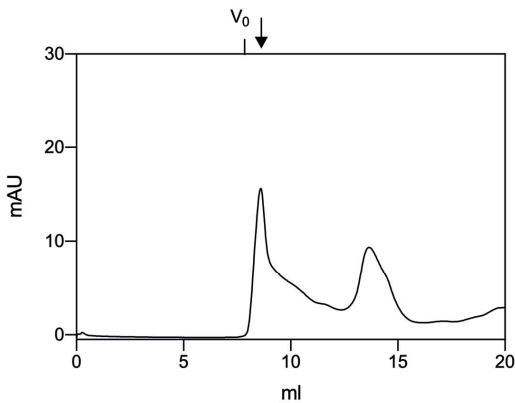
E



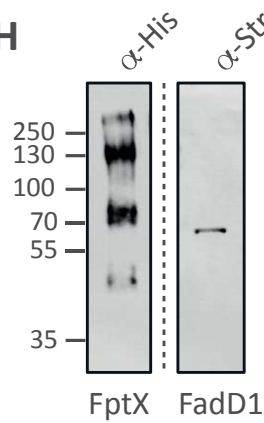
F



G



H



I

